MATERIAL SCIENCE Research Article ISSN: 2690-2532

Silver-incorporated TiO_2 Nanofibers via Electrospinning: An Efficient Antibacterial Agent

*Misbah Rasheed**

Department of Physics, Hazara University, Pakistan

***Corresponding author:**

Misbah Rasheed

Department of Physics, Hazara University, Mansehra, Dhodial, Pakistan, Phone: 09826283791; E-mail: misbahrasheed12@yahoo.com

Received : September 26, 2024
Published : December 19, 2024

ABSTRACT

Pure as well different concentrations of silver-loaded titanium dioxide (TiO2) nanofibers of uniform and smooth surfaces were prepared by the sol gel and Electro-spinning technique primarily consists of TiP/pvp. The mean diameter of the obtained nanofibers ranges between 20 nm and 120 nm. The effect of silver loading on the fiber size and crystal structure was investigated. Post-calcination of nanofibers mats on 500°C resulted from the rutile phase to the anatase phase transformation. The effect of temperature (500°C was also studied on the size and morphology of the nanofibers. The structural, morphological, compositional, and optical properties were investigated by using X-ray diffraction (XRD), scanning electron microscopy (SEM), and UV-Vis absorption spectroscopy. In addition to this, the antibacterial effect of pure TiO_2 and Ag-loaded TiO_2 nanofibers were also studied against E. coli. and S. aureus. by using the Kirby Bauer method.

Keywords: Electrospinning, Titanium Dioxide, Loading, Nanofibers.

INTRODUCTION

Titanium dioxide (TiO_2) is one of the wide band gap semiconductor used in sensors, antibacterial agents, self-cleaner, water purification, transparent electrode, and other optoelectronic devices [1,2]. TiO_2 exists in three crystalline phases rutile phase, anatase phase, and brookite phase, but most common crystalline polymorphs of TiO_2 are metastable A and stable R-phases. The anpresence of either or both of these crystalline phases impacts the antibacterial performance of TiO_2. A-phase has been reported to have a lower surface enthalpy and surface free energy than R-phase. Rutile and anatase have tetragonal structures while brookite has the orthorhombic structure [3]. The rutile phase is widely used in cosmetics, ultraviolent (UV) absorbance, and high-quality paints because of its high refractive index and UV absorbance

[4]. Anatase phase is an optically and electrically +active and can be used an antibacterial agent, solar cells, in photonic devices and photo-catalysis [5]. titanium dioxide can be synthesized in the form of powder, thin films, etc. Thin films of TiO_2 can be prepared by the gas phase method. The important techniques are Chemical Vapor Deposition (CVD) [6], Spray Pyrolysis Deposition (SPD) [7] and Physical Vapor Deposition (PVD) [6].

Electro-spinning is a widely used technique to synthesize nanofibers. In this research work, TiO2/PVP, a hydrophilic polymer composite nanofiber was prepared by the sol-gel method combining with electrospinning technique. Specifically, the photocatalytic nature of titanium dioxide has made it's the best candidate of antimicrobial agent because it is a non-toxic, chemically stable, low cost, and Generally Recognized as Safe (GRAS) substance. Moreover, the silver/anatase composite nanofibers exhibited an excellent antibacterial rather than pure TiO_2 nanofibers [8].

The aim of this research work is to study the effect of silver (Ag) on the morphology, crystal structure and optical band gap of TiO_2 nanofibers. Silver ions continuously release silver ions which play an important role in killing the bacteria; therefore, antibacterial properties of TiO_2 have also been studied against *E. coli and S. aureus.*

Experimental

For the electrospinning suspension, 1.5 ml of titanium (IV) isopropoxide was mixed with 3 ml of acetic acid and left on stirring for 30 min continuously at room temperature, named as solution 1. In parallel, sliver nitrate ($AgNO_3$), 3 ml of DMF and 0.6 g of PVP (MW is 189,000) was added to 7 ml of ethanol and stirred for 15 min, named as solution 2. The solution 2 and solution 1 are mixed with four different loading concentration (0, 5, 10 and 15 wt % of the TiP) of silver nitrate for the electrospinning. Finally, the mixed solutions put on the stirrer for one hour. The as-prepared solution was used for the electrospinning to prepare nanofibers.

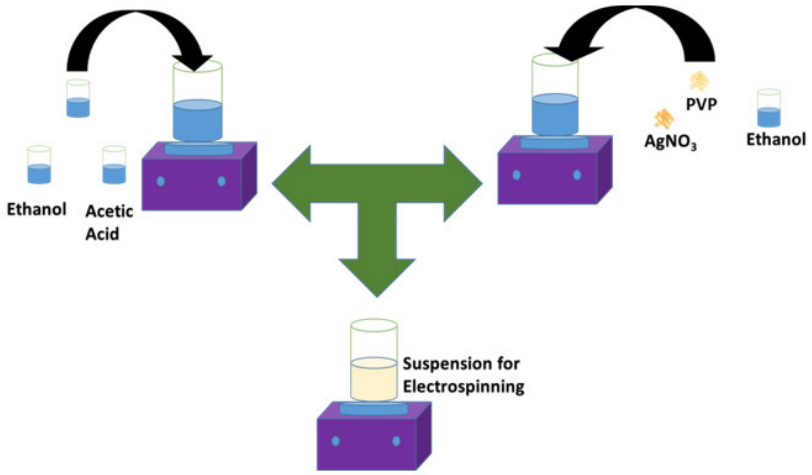

Figure 1. Schematic of the material synthesis.

The suspension was loaded into a syringe with a 26-gauge metallic needle. The high voltage D.C. power supply capable to generate 50 kV (Del Electronics Crop) was connected at the tip of the needle. The feeding rate was controlled by using a microcontroller. The feeding rate was kept at 1 ml/hr. The collector's copper plate was wrapped with aluminum foil and the distance between the tip of the syringe and the collector was kept at 14 cm to collect the nanofibers. An electrical field (20 kV) is applied between the syringe metallic needle and the grounded collector by the use of a high voltage supply. As the strength of the applied field increases, the curved surface of the fluid at the needle tip of the capillary tube stretches to form a cone known as the T- cone or Taylor cone [9,10]. The highly impermeable nanofibers are collected at a grounded collector, woven as well as non-woven mats [11,12]. The prepared nanofibers were left in the air for at least 3 hours to dry and complete the hydrolysis of TiP. In the end, the as-spun nanofibers were calcined in a furnace at temperature To

The suspension was loaded into a syringe with a 26-gauge metallic needle. The high voltage D.C. power supply capable to generate 50 kV (Del Electronics Crop) was connected at the tip of the needle. The feeding rate was controlled by using a microcontroller. The feeding rate was kept at 1 ml/hr. The collector's copper plate was wrapped with aluminum foil and the distance between the tip of the syringe and the collector was kept at 14 cm to collect the nanofibers. An electrical field (20 kV) is applied between the syringe metallic needle and the grounded collector by the use of a high voltage supply. As the strength of the applied field increases, the curved surface of the fluid at the needle tip of the capillary tube stretches to form a cone known as the T- cone or Taylor cone [9,10]. The highly impermeable nanofibers are collected at a grounded collector, woven as well as non-woven mats [11,12]. The prepared nanofibers were left in the air for at least 3 hours to dry and complete the hydrolysis of TiP. In the end, the as-spun nanofibers were calcined in a furnace at temperature 500°C with 5°C/min for three hours for to remove PVP and other unwanted species.

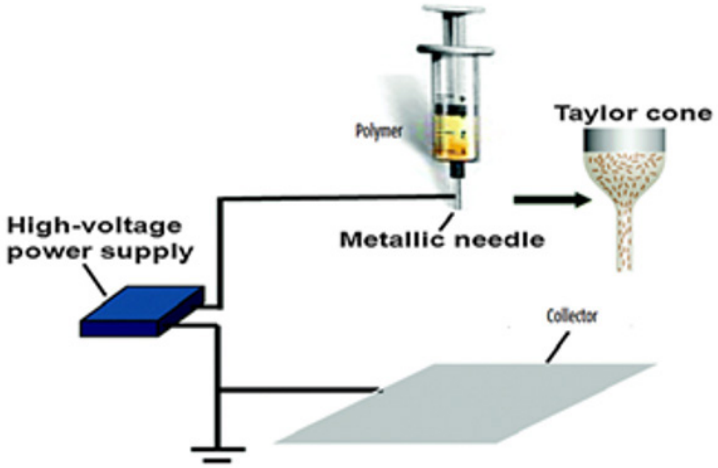

Figure 2. Vertical Arrangement for Electro-spinning.

The surface morphology and the elemental analysis of the nanofibers were studied by using scanning electron microscopy (Format Jeo/Eo, versioin1.1) equipped with EDX. The crystal phases of the nanofibers were observed by using an X-rays diffractometer (MIA Cu Kα radiative source). The Optical band gaps of the Ag-loaded TiO_2 nanofibers were studied by using UV-vis spectroscopy. Raman spectroscopy was used to study molecular interactions, chemical structure, phase and polymorph of the nanofibers. Antibacterial test was done by using Kirby-Bauer technique.

RESULTS AND DISCUSSION

SEM Analysis

SEM micrographs in Figure 3 confirm the formation of continuous and thin long nanofibers. The surface of Ag-loaded TiO_2 nanofibers is rough compared to pure TiO_2 nanofibers. The diameter of silver loaded TiO_2 nanofibers decreased because Ag-loaded TiO_2 has only the anatase phase which has a smaller grain size as compared to the rutile phase. Moreover, the diameter of calcinated nanofibers is small as compared to the as-spun nanofibers due to elimination of PVP, ethanol, rearrangement of atoms, the disintegration of TiP, and the subsequent sintering [13].

It is shown in micrographs that dendrite like structures were grown on the nanofibers surfaces which are due to the silver ions over the entire surface. These dendrites like structures have also been reported for other metals like copper, gold, zinc and silver as well and have been analyzed for different materials like ceramic, polymers, etc. [14,15].

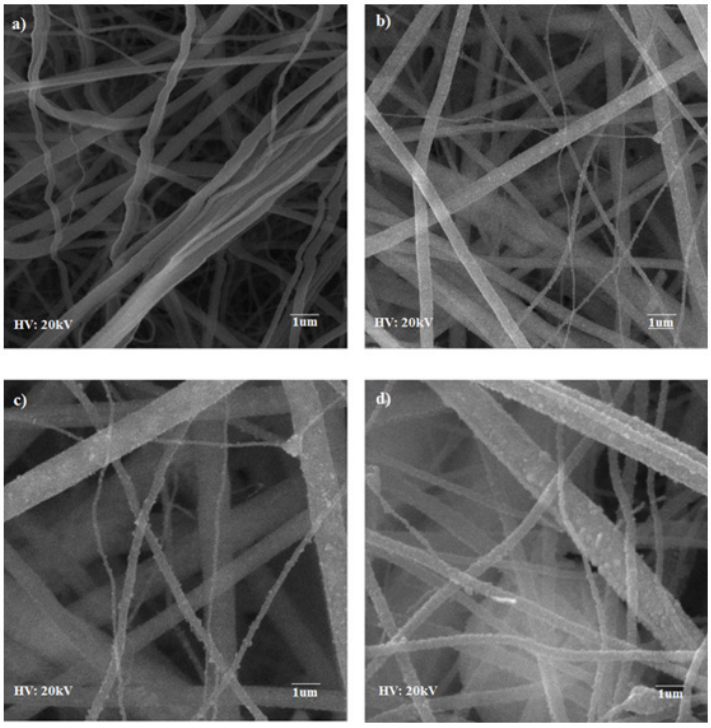

Figure 3. SEM micrographs of Calcined nanofibers at 500°C a) Pure TiO_2 b) 5 wt % Ag c) 10 wt % Ag d) 15 wt % Ag loaded TiO_2 nanofibers.

To confirm the Ag particles are present in the TiO2 nanofibers, Energy dispersive X-ray spectroscopy (EDX) has been used at different points of the nanofibers and obtained different concentrations of the silver in fibers shown in Figure 4. According to EDX the fiber composition of each element is shown in the table 1 below:

Table 1. Percentage composition of each element in the electrospun nanofibers calcined at 500 °C

Samples	Ti (%)	Oxygen (%)	Silver %
Pure TiO_2	59.3	40.3	0
5 wt % Ag-TiO_2	85.1	10.6	4.3
10 wt % Ag-TiO_2	51.8	40.8	7.8
15 wt % Ag-TiO_2	52.6	27.7	21.6

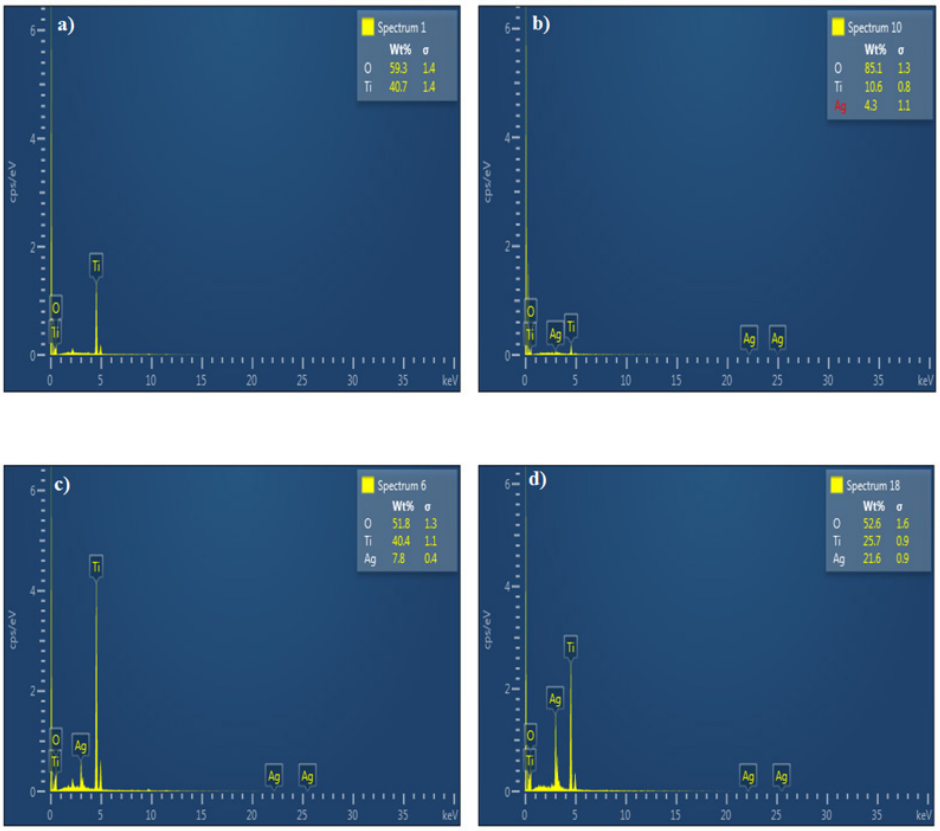

Figure 4. EDX spectroscopy pattern of calcined nanofibers at 500°C a) Pure TiO_2 b) 5 wt %Ag c) 10 wt % Ag d) 15 wt % Ag loaded TiO_2 nanofibers.

X-ray Diffraction

X-ray diffraction (XRD) is used to study the crystallographic structure, orientation of the planes and the identification of crystalline materials [16]. From the Figures, it was found that both anatase and rutile phases are present in the pure TiO_2, but as the concentration of Ag increased the rutile phase disappeared. The fact is that due to pinning of domain boundaries the domain mobility is limited by crystal defects [17]. The un-dissolved silver particles remain at the grain boundaries leading to reduce the particle contact and restrict them from grain growth and phase transition. Thus, silver content restricted the anatase phase to rutile phase transformation. Ag-loaded TiO_2 nanofibers has a larger crystallite size than the pure TiO_2 nanofibers. Seery et al. reported that the silver ion has a larger radius of 130 pm compared to the 68 pm of TiO_2, therefor Ag particles remain at the surface, preventing the phase transformation [18]. As the Ag concentration increased, dislocation density also increased. The dislocation density can be determined by using the formula $\sigma = 1/D2$ lines/nm2. In the Figure 5, the diffraction peaks at 25.63°, 44.54°, 64.79°, and 77.96° corresponds to the planes of (101), (002), (312), and (103) respectively, which represent the formation of anatase phases of Titania. The peak of rutile phase can be seen at 38.29° and 47.6° respectively, which are associated with the lattice planes of (211) and (303) (PDF number 01-083-2243). In Figure 5-d diffraction peaks of metallic silver at 77.76o and 82.19o and were produced with crystal planes of (022) and (222) which were confirmed by the (PDF number 01-073-1774).

REFERENCES

1. Boyle VJ, Fancher ME, Ross RW Jr. (1973). Rapid, modified Kirby-Bauer susceptibility test with single, high-concentration antimicrobial disks. Antimicrob Agents Chemother. 3(3):418-424.

2. Carp O, Huisman CL, Reller A. (2004). Photoinduced reactivity of titanium dioxide. Progress in solid state chemistry. 32(1-2):33-177.

3. Doh SJ, Kim C, Lee SG, Lee SJ, Kim H. (2008). Development of photocatalytic TiO2 nanofibers by electrospinning and its application to degradation of dye pollutants. J Hazard Mater. 154(1-3):118-127.

4. Wang C, Ao Y, Wang P, Hou J, Qian J, Zhang S. (2010). Preparation, characterization, photocatalytic properties of titania hollow sphere doped with cerium. J Hazard Mater. 178(1-3):517-521.

5. Soo JZ, Chai LC, Ang BC, Ong BH. (2020). Enhancing the Antibacterial Performance of Titanium Dioxide Nanofibers by Coating with Silver Nanoparticles. ACS Appl Nano Mater. 3:5743-5751.

6. Hashimoto K, Irie H, Fujishima A. (2005). TiO2 photocatalysis: a historical overview and future prospects. Japanese journal of applied physics. 44(12R):8269.

7. Hidalgo M, Aguilar M, Maicu M, Navío JA, Colón G. (2007). Hydrothermal preparation of highly photoactive TiO2 nanoparticles. Catalysis Today. 129(1-2):50-58.

8. Giolli C, et al. (2007). Characterization of TiO2 coatings prepared by a modified electric arc-physical vapour deposition system. Surface and Coatings Technology. 202(1):13-22.

9. Li Z, Wang C. (2013). Effects of working parameters on electrospinning. In One-dimensional nanostructures: Springer. pp. 15-28.

10. Yang Y, Jia Z, Liu J, Li Q, Hou L, Wang L, et al. (2008). Effect of electric field distribution uniformity on electrospinning. Journal of applied physics. 103(10):104307.

11. Al-Hazeem NZA. (2018). Nanofibers and electrospinning method. Nanomater.-Synth. Appl.

12. Angammana CJ, Jayaram SH. (2011). The Effects of Electric Field on the Multijet Electrospinning Process and Fiber Morphology. IEEE Trans Ind Appl. 47:1028-1035.

13. Li D, Xia Y. (2003). Fabrication of titania nanofibers by electrospinning. Nano letters. 3(4):555-560.

14. Fang J, Ding B, Song X, Han Y. (2008). How a silver dendritic mesocrystal converts to a single crystal. Applied Physics Letters. 92(17):173120.

15. Govenius J, Lake R, Tan K, Möttönen M. (2016). Detection of zeptojoule microwave pulses using electrothermal feedback in proximity-induced Josephson junctions. Physical review letters. 117(3):030802.

16. Chauhan A, Chauhan P. (2014). Powder XRD technique and its applications in science and technology. J Anal Bioanal Tech. 5(5):1-5.

17. Raffi M, et al. (2018). Synthesis of Ag-loaded TiO2 electrospun nanofibers for photocatalytic decolorization of methylene blue. Fibers and Polymers. 19(9):1930-1939.

18. Pelaez M, et al. (2012). A review on the visible light active titanium dioxide photocatalysts for environmental applications. Applied Catalysis B: Environmental. 125:331-349.

19. Feng X, Wang X, Chen X, Yue Y. (2011). Thermo-physical properties of thin films composed of anatase TiO2 nanofibers. Acta Materialia. 59(5):1934-1944.

20. Biemer JJ. (1973). Antimicrobial susceptibility testing by the Kirby-Bauer disc diffusion method. Ann Clin Lab Sci (1971). 3(2):135-140.

21. Wang L, Ali J, Zhang C, Mailhot G, Pan G. (2020). Simultaneously Enhanced Photocatalytic and Antibacterial Activities of TiO2/Ag Composite Nanofibers for Wastewater Purification. J Environ Chem Eng. 8:102104.

22. Fabrega J, Fawcett SR, Renshaw JC, Lead JR. (2009). Silver nanoparticle impact on bacterial growth: effect of pH, concentration, and organic matter. Environ Sci Technol. 43:7285-7290.

23. Sanjines R, Tang H, Berger H, Gozzo F, Margaritondo G, Levy F. (1994). Electronic structure of anatase TiO2 oxide. Journal of Applied Physics. 75(6):2945-2951.

Citation: Rasheed M. (2024). Silver-incorporated TiO2 Nanofibers via Electrospinning: An Efficient Antibacterial Agent. Material Science. 6(2):36.

DOI : https://doi.org/10.35702/msci.10036